VIP Carbon Nanotubes

DOI: 10.1002/ange.200902468

# Experimentally Determined Redox Potentials of Individual (*n*,*m*) Single-Walled Carbon Nanotubes**

*Yasuhiko Tanaka, Yasuhiko Hirana, Yasuro Niidome, Koichiro Kato, Susumu Saito, and Naotoshi Nakashima**

Ever since the discovery of carbon nanotubes (CNTs), many groups have endeavored to understand the fundamental properties of the CNTs. The redox properties (i.e. electronic densities, the Fermi levels, redox potentials) of single-walled carbon nanotubes (SWNTs) are related to the structures of SWNTs that have a specified diameter and chirality angle uniquely related to a pair of integers (*n*,*m*); the so-called chiral indices.[1,2] Many attempts have been made to determine the electronic properties of SWNTs using scanning tunneling spectroscopy,[3] redox titrimetry,[4] photoluminescence (PL) measurements,[5–7] and spectroelectrochemistry;[8–13] however, the success in the determination of the redox properties as already reported has been low. Recently, Paolucci et al.[12] employed Vis–near-IR absorption spectroelectrochemistry to estimate the redox potentials of the SWNTs dissolved in an ultradry dimethylsulfoxide (DMSO) solution; however, it is not easy to determine the redox potentials of isolated (*n*,*m*)SWNTs using this method because SWNTs with several different chiral indices have band gaps in the near-IR region that overlap one another. We now describe a simple method for the determination of the redox potentials of many (in this study, fifteen) individual (*n*,*m*)SWNTs using near-IR PL spectroelectrochemistry in an aqueous medium.

[*] Dr. Y. Tanaka, Y. Hirana, Prof. Y. Niidome, Prof. Dr. N. Nakashima
Department of Applied Chemistry, Graduate School of Engineering, Kyushu University
Motooka 744, Fukuoka 819-0395 (Japan)
Fax: (+81) 92-802-2840
E-mail: nakashima-tcm@mail.cstm.kyushu-u.ac.jp
Prof. Dr. N. Nakashima
Japan Science and Technology -CREST
5 Sanbancho, Chiyoda-ku, Tokyo, 102-0075 (Japan)
K. Kato, Prof. Dr. S. Saito
Department of Physics,Tokyo Institute of Technology
2-12-1, Oh-okayama, Meguro-ku, Tokyo (Japan)

[**] We thank Prof. Mildred S. Dresselhaus of Massachussets Institute of Technology for her consideration and comments on this paper, and Professors F. M. Hawkridge of Virginia Commonwealth University and T. Sagara of Nagasaki University for helpful discussions. This work was supported by a Grant-in-Aid for Scientific Research (A) (No.17205014 for N.N.), Priority Areas "Super-Hierarchical Structures" (No.19022030 for N.N.) and "Carbon Nanotube Nanoelectronics" (No. 19054005 for S.S.), the Global COE Program "Science for Future Molecular Systems" (Kyushu University) and "Nanoscience and Quantum Physics" (Tokyo Institute of Technology), and Nanotechnology Network Project (Kyushu-area Nanotechnology Network) from the Ministry of Education, Culture, Sports, Science and Technology (Japan).

Supporting information for this article is available on the WWW under http://dx.doi.org/10.1002/anie.200902468.

Strategic approaches toward the solubilization of CNTs are essential for many applications of CNTs[14] and numerous dispersants including carboxymethylcellulose sodium salt (CMC, Figure S1a in the Supporting Information)[15] have been used to individually dissolve SWNTs. In this study, we fabricated a non-fluorescent transparent indium tin oxide (ITO) electrode modified with a cast film of CMC/poly-(diallyldimethylammonium chloride) (PDDA; Figure S1b in the Supporting Information) that contained isolated SWNTs (for details, see Experimental Section in the Supporting Information).

We have discovered that we can determine the redox potentials of isolated SWNTs having their own chirality indices by in situ near-IR PL spectroelectrochemistry at the fabricated modified ITO electrode. This modified film retains the isolated SWNTs and the spectroelectrochemical results are analyzed with the Nernst equation.

Externally applied potentials were changed in the range of $-1.0$–$+1.1$ V versus Ag|AgCl (saturated KCl) in 0.3 M aqueous NaCl containing 30 mM $Na_2HPO_4$ (pH 8) because in this potential range, both CMC and PDDA are electroinactive. The open circuit potential (OCP) of the modified electrode was around 0.0 V, which is almost identical with the OCP value[8b] of a bundled SWNT film on an electrode. Herein, neutral SWNTs are denoted as $SWNT^0$. The $SWNT^0$ were changed into reduced form (denoted as $SWNT^{n-}$) and oxidized form ($SWNT^{n+}$) when the external potential was applied to the electrode in arbitrary steps from 0.0 V to $-1.0$ V and from 0.0 V to $+1.1$ V, respectively. After each potential step, the applied potential was returned to 0.0 V and it was confirmed that no significant spectral change in the SWNT had occurred, namely, the SWNTs in the film are stable during these electrochemically driven redox processes. This behavior of the SWNTs is consistent with those in Vis–near-IR absorption[8b] and Raman[10b] spectroelectrochemical studies.

We carried out in situ near-IR absorption spectroelectrochemistry using the modified electrode. The near-IR absorption spectra of the individually solubilized SWNTs were found to bleach when the external potential was applied to the electrode by a step from 0.0 V to $-1.0$ V (see the Supporting Information, Figure S2a) and from 0.0 V to $+1.1$ V (see, Figure S2b). Unfortunately, the determination of the redox potentials of individual SWNTs having their own chirality indices was difficult because the near-IR absorption peaks from the SWNTs with several different chirality indices have band gaps that overlap one another (see Supporting Information).

The PL of SWNTs is consistent with isolated SWNTs and therefore characterization of isolated SWNTs is possible. Individual SWNTs dissolved in a surfactant solution exhibit PL in the near-IR region,[16] and the chiralities of the SWNTs can be determined by contour two-dimensional (2D) PL mapping. The surface and 2D plots of PL intensity as a function of emission and excitation wavelengths for the modified film on ITO are shown in Figure 1, in which we see

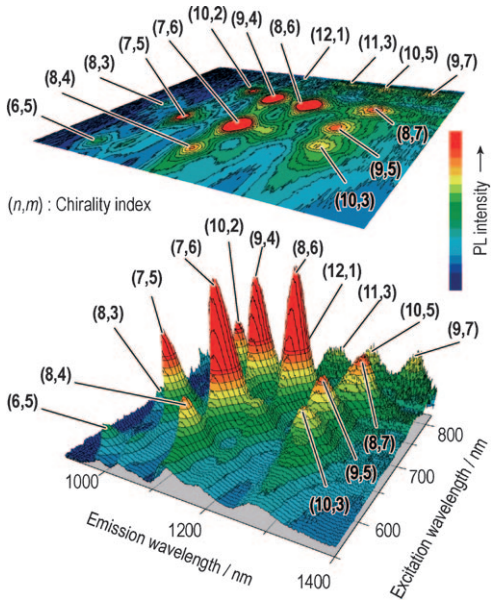


***Figure 1.*** Surface and 2D plots of PL intensity as a function of emission and excitation wavelengths. The data were obtained for a film of SWNTs/CMC/PDDA on an ITO electrode in 0.3 M aqueous NaCl containing 30 mM $Na_2HPO_4$ (pH 8).

fifteen individual SWNTs having chirality indices of (6,5), (8,3), (7,5), (8,4), (10,2), (7,6), (9,4), (10,3), (8,6), (9,5), (12,1), (11,3), (8,7), (10,5), and (9,7). We carried out in situ near-IR PL spectroelectrochemistry in a way similar to the in situ near-IR absorbance spectroelectrochemistry method described above. As typical examples, in Figure 2, we show the PL spectra of the SWNTs having (7,5), (7,6), (10,3), (12,1), (11,3), (10,5), and (9,7) chirality indices at applied potentials from 0.0 to −1.0 V and then from 0.0 to +1.1 V (for the other eight SWNTs with chirality indices of (6,5), (8,3), (8,4), (10,2), (9,4), (9,5), (8,6), and (8,7), see Figures S3 and S4 in the Supporting Information). It is evident that the PL spectra show a strong dependence on the applied potential.

For the results of the potential-dependent PL responses (see Figure 2, and Figure S3 and S4 in the Supporting Information), we plotted ΔPL values of fifteen isolated SWNTs as a function of applied potentials in Figure 3 and fitted using nonlinear regression[12] with the Nernst equations Equations (1) and (2)

$$\Delta PL_{red} = \frac{1}{1+\exp\left[\frac{nF}{RT}(E^{0'}_{red}-E)\right]} \quad (1)$$

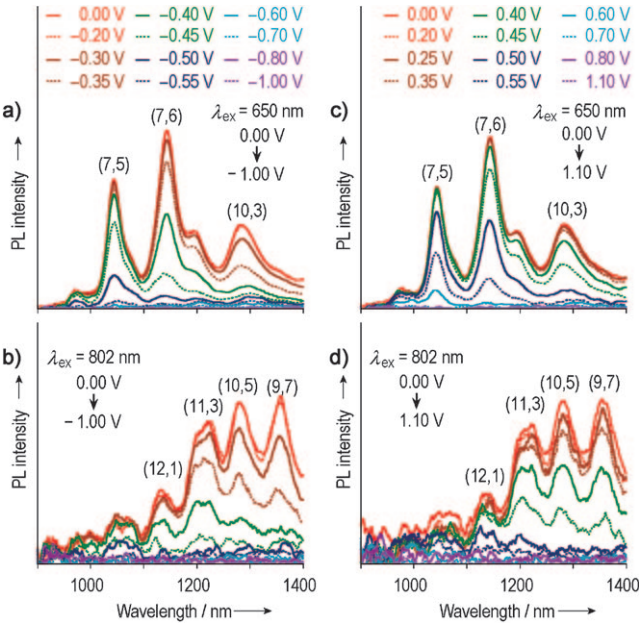


***Figure 2.*** Dependence of the PL spectra (of the film containing isolated SWNTs on an ITO electrode) on the external applied potential. a) and c) PL spectra excited at 650 nm, in which signals for (7,5), (7,6), and (10,3) SWNTs appear. b) and d) PL spectra excited at 802 nm, in which signals for (12,1), (11,3), (10,5), and (9,7) SWNTs appear. In this experiment, the potential was applied to the electrode from 0.0 V to −1.0 V (a and b) and from 0.0 V to +1.1 V (c and d).

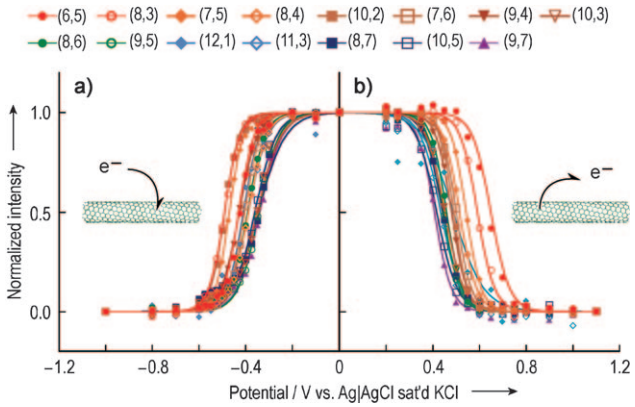


***Figure 3.*** Normalized PL intensity of the film containing fifteen isolated SWNTs on an ITO electrode as a function of external applied potential showing the Nernst analysis curves (each solid line) of the experimental results. In the experiment, a potential was applied to the electrode from 0.0 V to −1.0 V (a) and from 0.0 V to +1.1 V (b).

$$\Delta PL_{ox} = \frac{1}{1+\exp\left[\frac{nF}{RT}(E-E^{0'}_{ox})\right]} \quad (2)$$

where $\Delta PL_{red}$ and $\Delta PL_{ox}$ is the ratio of $SWNT^0$ (assumed as $\Delta PL_{red} = SWNT^0/(SWNT^0 + SWNT^{n-})$ and $\Delta PL_{ox} = SWNT^0/(SWNT^0 + SWNT^{n+})$, respectively), $F$ is the Faraday constant, $n$ is the number of electrons transferred during the reaction, $R$ is the gas constant, $T$ is the absolute temperature (298.15 K), $E^{0'}_{red}$ and $E^{0'}_{ox}$ are the formal potential and $E$ is the applied

electrode potential (also see Figures S5 and S6 in the Supporting Information, the plots of normalized PL intensity versus applied potentials for each SWNT with its own chirality index). The correlation coefficients ($R^2$ values) for the Nernst fitting were 0.983–0.999, indicating that the experimental data are in good agreement with the Nernst equation analysis. We have observed steeper changes in the regression curves of the potential-dependent PL changes than for the absorption spectral responses.

This result is reasonable because the potential dependence on the PL intensity is due to the isolated SWNTs, whereas the absorption spectral response is due to SWNTs with several different chirality indices. Note that the Nernst analysis is applicable for all isolated SWNTs. The plots of ΔPL show inflection points from which we can easily determine the formal potentials of the fifteen isolated SWNTs to be: 1) for the reduction process ($E^{0'}_{red}$), −0.43, −0.49, −0.47, −0.39, −0.49, −0.41, −0.43, −0.35, −0.39, −0.34, −0.41, −0.39, −0.35, −0.36, and −0.34 V versus Ag | AgCl (saturated KCl) and 2) for the oxidation process ($E^{0'}_{ox}$), 0.64, 0.59, 0.54, 0.52, 0.49, 0.50, 0.48, 0.45, 0.46, 0.45, 0.49, 0.44, 0.44, 0.42, and 0.41 V versus Ag | AgCl (saturated KCl) on the SWNTs with chirality indices of (6,5), (8,3), (7,5), (8,4), (10,2), (7,6), (9,4), (10,3), (8,6), (9,5), (12,1), (11,3), (8,7), (10,5), and (9,7), respectively, which are presented in Figure 4a, in which mod $(2n+m,\ 3)=1$ ("mod 1") and mod $(2n+m,\ 3)=2$ ("mod 2") are plotted separately. As can be seen in Figure 4a, mod 2 SWNTs gave somewhat smaller band gaps than those of mod 1 SWNTs. The difference in solvation between the mod 1 and mod 2 may explain this behavior, however the exact cause is not clear at present.

Optical transition energies, namely the optical band gaps ($\Delta E_{opt}$), of the isolated SWNTs can be obtained from the PL spectra and the values are plotted in Figure 4b as the blue inverted triangles. We also determined electrochemical band gaps ($\Delta E_{electr} = E^{0'}_{red} - E^{0'}_{ox}$) and the Fermi levels ($E_f$, here $E_f = (E^{0'}_{red} + E^{0'}_{ox})/2$) of the fifteen isolated SWNTs from $E^{0'}_{red}$ and $E^{0'}_{ox}$; the $\Delta E_{electr}$ (Figure 4b, red triangles) are: 1.07, 1.08, 1.01, 0.91, 0.98, 0.91, 0.91, 0.81, 0.85, 0.79, 0.90, 0.82, 0.79, 0.78, and 0.75 eV and the $E_f$ (Figure 4a, diamonds) are: 0.11, 0.05, 0.04, 0.06, 0.00, 0.05, 0.03, 0.05, 0.03, 0.05, 0.04, 0.02, 0.05, 0.03, and 0.03 V versus Ag | AgCl (saturated KCl) for the SWNTs with chirality indices of (6,5), (8,3), (7,5), (8,4), (10,2), (7,6), (9,4), (10,3), (8,6), (9,5), (12,1), (11,3), (8,7), (10,5), and (9,7), respectively.

As shown in Figure 4b, the difference between the two band gaps, $\Delta E_{electr}$ and $\Delta E_{opt}$, was approximately 0.16–0.21 eV. Excitonic binding energy is essentially important to understand the optical band gap of SWNTs. Excitonic binding energy is explained by the interaction between a hole and an electron that are generated by photoexcitation of an isolated SWNT;[17] thus; the exciton does not accompany charge transfer from/to the SWNTs. On the other hand, for understanding the $\Delta E_{electr}$, the solvation of reduced/oxidized SWNTs as well as the counterions of the charged SWNTs should be taken into account. Thus, $\Delta E_{electr}$ values depend on the solvent properties. Paolucci et al.[12] estimated the redox potentials for the isolated SWNTs in dimethylsulfoxide (DMSO) using absorption spectroelectrochemistry (see Figure S7 in the Supporting Information). The Fermi levels of the isolated SWNTs obtained in the present study (aqueous medium) and those reported (in DMSO) were similar to each other, but the $\Delta E_{electr}$ values in the aqueous system were lower

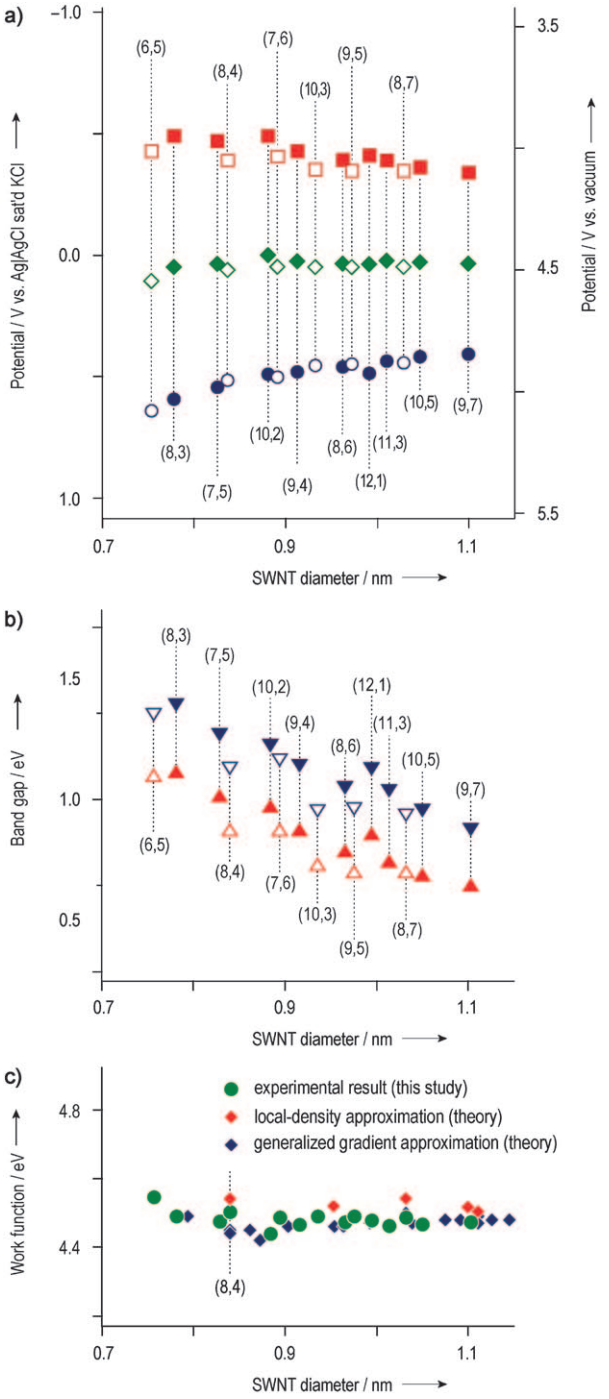


***Figure 4.*** a) Oxidation (blue circles), reduction (red squares), and Fermi level (green diamonds) potentials of fifteen isolated SWNTs. b) Optical (inverted blue triangles) and the electrochemical (red triangles) band gap determined by the experiment. In (a) and (b) solid symbols represent mod 1 and open symbols represent mod 2, respectively. c) Comparison of the present study (green circles), theory (local-density approximation (red diamonds), and generalized gradient approximation from ref. [18b] (blue diamonds).

than those in the DMSO system. This situation is consistent with our consideration of the solvation of the SWNTs; that is, the lower $\Delta E_{electr}$ values in the aqueous system are probably due to the higher solvation energy of the reduced/oxidized SWNTs.

The work functions (WFs) of SWNTs can be obtained by first-principles electronic-structure calculations. It has been reported that the WFs of SWNTs having the diameters larger than 1 nm lie within a narrow distribution and show no significant chirality nor diameter dependence, while for SWNTs with the diameters smaller than 1 nm, the WFs show a sizable chirality as well as diameter dependence.[18] The WFs of this system are obtained from the Fermi energy and the equation[19] of potential scale versus the vacuum level, $E\,(\mathrm{V\ vs.\ vacuum}) = E\,(\mathrm{V\ vs.\ SHE}) + 4.24\,(\mathrm{V})$ (SHE = standard hydrogen electrode potential). The redox properties of the fifteen individual SWNTs are summarized in Table 1. As can be seen in Figure 4a, the chirality dependence of the

***Table 1:*** Experimentally determined redox properties of fifteen isolated SWNTs.

| Chirality index (*n*,*m*) | Nanotube diameter [nm] | $E_{ox}^{0'}$ [V vs. vacuum] | $E_{red}^{0'}$ [V vs. vacuum] | $E_f$ [V vs. vacuum] | $\Delta E_{electr}$ [eV] |
|---|---|---|---|---|---|
| (6,5) | 0.757 | 5.08 | 4.01 | 4.55 | 1.07 |
| (8,3) | 0.782 | 5.03 | 3.95 | 4.49 | 1.08 |
| (7,5) | 0.829 | 4.98 | 3.97 | 4.48 | 1.01 |
| (8,4) | 0.840 | 4.96 | 4.05 | 4.50 | 0.91 |
| (10,2) | 0.884 | 4.93 | 3.95 | 4.44 | 0.98 |
| (7,6) | 0.895 | 4.94 | 4.03 | 4.49 | 0.91 |
| (9,4) | 0.916 | 4.92 | 4.01 | 4.47 | 0.91 |
| (10,3) | 0.936 | 4.89 | 4.09 | 4.49 | 0.81 |
| (8,6) | 0.966 | 4.90 | 4.05 | 4.47 | 0.85 |
| (9,5) | 0.976 | 4.89 | 4.09 | 4.49 | 0.79 |
| (12,1) | 0.995 | 4.93 | 4.03 | 4.48 | 0.90 |
| (11,3) | 1.014 | 4.87 | 4.05 | 4.46 | 0.82 |
| (8,7) | 1.032 | 4.88 | 4.09 | 4.49 | 0.79 |
| (10,5) | 1.050 | 4.86 | 4.08 | 4.47 | 0.78 |
| (9,7) | 1.103 | 4.85 | 4.10 | 4.47 | 0.75 |

oxidation potentials seems to be slightly larger than that of the reduction potentials; especially, the $v_1$ level of the tubes whose diameters are smaller than approximately 0.85 nm shows stronger chirality dependence. The theoretical prediction described below explains this behavior.

In addition to the theoretical WFs reported in the literature, we have calculated the WFs of several SWNTs, (8,4), (8,8), (12,0), (13,0), and (14,0) in the framework of the density-functional theory (DFT) using the Quantum ESPRESSO.[20] In this first-principles study of WFs, we have completely optimized the geometrical parameters including the lattice constant. In Figure 4c, we show the WFs from theory and our experimental results. It is evident that the theory and our experimental data show similar tendencies, namely the WFs of SWNTs whose diameters are larger than 0.85 nm do not show significant chirality dependence, while the WFs of SWNTs whose diameters are smaller than 0.85 nm increased with a decrease in the tube diameters. It is interesting to note that in the case of the small-diameter (8,4) nanotube, our own data with the complete geometry optimization are found to be in excellent agreement with the experimental results. After the geometry optimization bond lengths for the three kinds of bonds in the chiral (8,4) nanotube are found to be different from each other, and are all slightly longer than the value of graphene (see Supporting Information). This result clearly indicates the importance of the complete geometry optimization in the case of thin SWNTs.

In conclusion, we have described an experimental method for determining the redox potentials of fifteen isolated SWNTs having their own chirality indices. The method is based on the Nernst analysis of the in situ PL spectroelectrochemical data of the isolated nanotubes. The WFs of the SWNTs obtained by our experimental analysis showed similar chirality dependence with those of the first-principle calculations (theory). We emphasize that the present method is very simple and is applicable to the determination of redox potentials of all isolated SWNTs whose PL detection is possible. Investigations using many different kinds of SWNTs are now underway in our laboratory. From the comparison of the work functions (WFs) obtained by the present method with those from first-principles electronic-structure theory, the importance of the geometrical optimization in small-diameter SWNTs is confirmed. It is also revealed that we can control the redox potentials of isolated SWNTs by fine-tuning the externally applied potential. The present study opens a door for the direct determination of the absolute potential of the energy levels of isolated SWNTs.

Received: May 9, 2009
Revised: July 18, 2009
Published online: September 8, 2009

**Keywords:** electrochemistry · nanotubes · photoluminescence · redox chemistry

[1] R. Saito, G. Dresselhaus, M. S. Dresselhaus, *Physical Properties of Carbon Nanotubes*, Imperial College Press, London, **1998**.
[2] N. Hamada, S. Sawada, A. Oshiyama, *Phys. Rev. Lett.* **1992**, *68*, 1579.
[3] J. W. G. Wilder, L. C. Venema, A. G. Rinzier, R. E. Smalley, C. Dekker, *Nature* **1998**, *391*, 59.
[4] M. Zheng, B. A. Diner, *J. Am. Chem. Soc.* **2004**, *126*, 15490.
[5] M. J. O'Connell, E. E. Eibergen, S. K. Doorn, *Nat. Mater.* **2005**, *4*, 412.
[6] A. Nish, R. J. Nicholas, *Phys. Chem. Chem. Phys.* **2006**, *8*, 3547.
[7] a) T. J. McDonald, D. Svedruzic, Y.-H. Kim, J. L. Blackburn, S. B. Zhang, P. W. King, M. J. Heben, *Nano Lett.* **2007**, *7*, 3528; b) T. J. McDonald, D. Svedruzic, Y.-H. Kim, J. L. Blackburn, S. B. Zhang, P. W. King, M. J. Heben, *Nano Lett.* **2008**, *8*, 1783.
[8] a) L. Kavan, P. Rapta, L. Dunsch, *Chem. Phys. Lett.* **2000**, *328*, 363; b) L. Kavan, P. Rapta, L. Dunsch, M. J. Bronikowski, P. Willis, R. E. Smalley, *J. Phys. Chem. B* **2001**, *105*, 10764; c) L. Kavan, L. Dunsch, *Electrochemistry of carbon nanotubes in Carbon Nanotubes: Advanced Topics in the Synthesis Structure, Properties and Applications*, *Vol. 111*, Springer, Berlin, **2008**.
[9] S. Kazaoui, N. Minami, N. Matsuda, H. Kataura, Y. Achiba, *Appl. Phys. Lett.* **2001**, *78*, 3433.

  

[10] a) K.-i. Okazaki, Y. Nakato, K. Murakoshi, *Phys. Rev. B* **2003**, *68*, 035434; b) K. Murakoshi, K.-i. Okazaki, *Electrochim. Acta* **2005**, *50*, 3069.
[11] P. Corio, A. Jorio, N. Demir, M. S. Dresselhaus, *Chem. Phys. Lett.* **2004**, *392*, 396.
[12] D. Paolucci, M. M. Franco, M. Iurlo, M. Marcaccio, M. Prato, F. Zerbetto, A. Penicaud, F. Paolucci, *J. Am. Chem. Soc.* **2008**, *130*, 7393.
[13] C. Ehli, C. Oelsner, D. M. Guldi, A. Mateo-Alonso, M. Prato, C. Schmidt, C. Backes, F. Hauke, A. Hirsch, *Nat. Chem.* **2009**, *1*, 243.
[14] a) N. Nakashima, *Int. J. Nanosci.* **2005**, *4*, 119; b) H. Murakami, N. Nakashima, *J. Nanosci. Nanotechnol.* **2006**, *6*, 16; c) N. Nakashima, T. Fujigaya, *Chem. Lett.* **2007**, *36*, 692; d) N. Nakashima, T. Fujigaya, H. Murakami, *Soluble Carbon Nanotubes*, American Scientific Publisher, California, **2008**.
[15] N. Minami, Y. Kim, K. Miyashita, S. Kazaoui, B. Nalini, *Appl. Phys. Lett.* **2006**, *88*, 093123.
[16] a) M. J. O'Connell, S. M. Bachilo, C. B. Huffman, V. C. Moore, M. S. Strano, E. H. Haroz, K. L. Rialon, P. J. Boul, W. H. Noon, C. Kittrell, J. Ma, R. H. Hauge, R. B. Weisman, R. E. Smalley, *Science* **2002**, *297*, 593; b) S. M. Bachilo, M. S. Strano, C. Kittrell, R. H. Hauge, R. E. Smalley, R. B. Weisman, *Science* **2002**, *298*, 2361.
[17] a) C. D. Spataru, S. Ismail-Beigi, L. X. Benedict, S. G. Louie, *Phys. Rev. Lett.* **2004**, *92*, 077402; b) F. Wang, G. Dukovic, L. E. Brus, T. F. Heinz, *Science* **2005**, *308*, 838; c) O. Kiowski, S. Lebedkin, F. Hennrich, S. Malik, H. Rösner, K. Arnold, C. Sürgers, M. M. Kappes, *Phys. Rev. B* **2007**, *75*, 075421.
[18] a) B. Shan, K. Cho, *Phys. Rev. Lett.* **2005**, *94*, 236602; b) V. Barone, J. E. Peralta, J. Uddin, G. E. Scuseria, *J. Chem. Phys.* **2006**, *124*, 024709.
[19] C. P. Kelly, C. J. Cramer, D. G. Truhlar, *J. Phys. Chem. B* **2007**, *111*, 408.
[20] P. Giannozi, *Quantum ESPRESSO*, DEMOCRITOS, Udine-Trieste.

  